

DISLOCATION DENSITY BASED FINITE ELEMENT MODELING OF ULTRASONIC CONSOLIDATION

D. Pal and B. E. Stucker,

Utah State University, Logan, UT 84341

Reviewed, accepted September 23, 2010

Abstract

A dislocation density based constitutive model has been developed and implemented into a crystal plasticity quasi-static finite element framework. This approach captures the statistical evolution of dislocation structures and grain fragmentation at the bonding interface when sufficient boundary conditions pertaining to the Ultrasonic Consolidation process are prescribed.

Hardening is incorporated using statistically stored and geometrically necessary dislocation densities (SSDs and GNDs), which are dislocation analogs of isotropic and kinematic hardening respectively. The GND considers strain-gradient and thus renders the model size-dependent. The model is calibrated using experimental data from published refereed literature and then validated for the Aluminum 3003 alloy.

Introduction

As a direct result of ongoing research efforts in ultrasonic consolidation (UC) worldwide [1], it has become apparent that a new approach to modeling of UC bonding is needed. A model which provides a better understanding of the effects of process parameter changes on grain refinement, plastic deformation and bonding during UC will better enable researchers to predict which materials will bond, how the mechanical properties of UC-produced parts can be improved, and how to better design the next generation of UC equipment.

The continuum properties of parts made using UC are strongly dependent upon the micromechanics of the bonded interface [1]. Interfacial-scale microstructures can be studied fundamentally using electron microscopy [1] and can be used to correlate atomic and mesoscopic mechanisms of deformation to their continuum counterparts. A dislocation density-based crystal plasticity Finite Element Model (FEM) can capture the statistical distribution of dislocations, partials and various deformation mechanisms at the bonding interface as inputs to predict macroscopic deformation profiles as a function of energy input characteristics. These input characteristics are a function of the process parameters used in a UC machine, namely vibration amplitude, normal force, ultrasonic frequency, welding speed, sonotrode geometry and temperature.

Problem Formulation

It has been shown that material sheets subjected to UC undergo inhomogeneous plastic deformation through their thickness [1]. Classical continuum plasticity theories do not fully explain this phenomenon [2]. Therefore, a study of strain localization and grain refinement at the material interfaces during UC bonding is required. The following steps lead to the calculation of these localized strains and their effects.

Large Deformation Quasi-Static Crystal Plasticity Description

The deformation map in space and time is described by the total deformation gradient tensor \mathbf{F} (Figure 1). Applying the Kroner-Lee assumption, \mathbf{F} is decomposed into elastic \mathbf{F}^e and plastic gradient \mathbf{F}^p tensors using multiplicative operator theory

$$F = F^e F^p \quad (\text{Eqn 1})$$

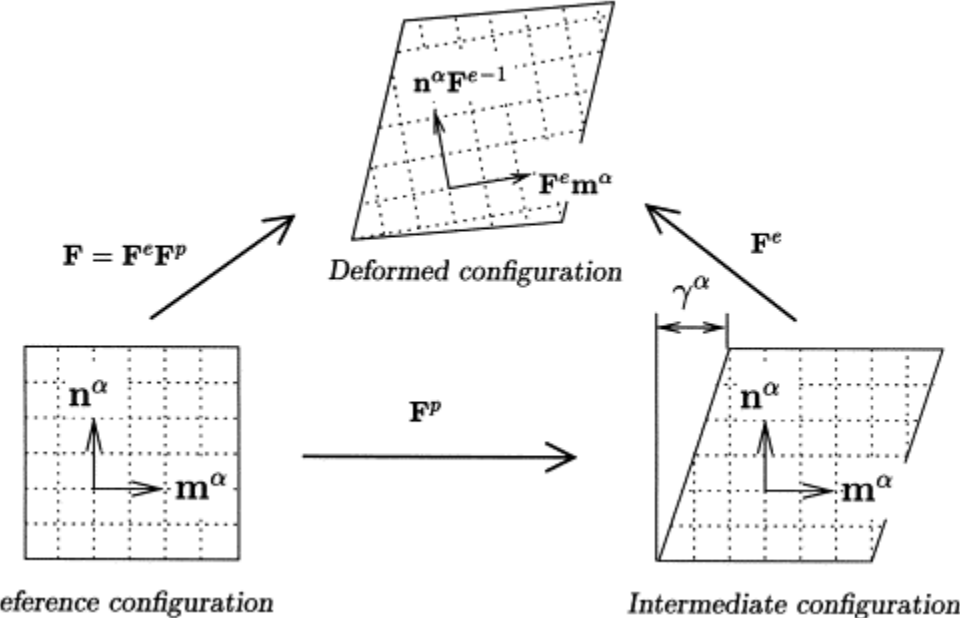


Figure 1 Multiplicative decomposition of the total deformation gradient, $\mathbf{F}=\mathbf{F}^e\mathbf{F}^p$. The rotation and stretching of the lattice are taken into account through the elastic deformation gradient \mathbf{F}^e [4].

The plastic deformation gradient \mathbf{F}^p includes the constant volume plastic deformation without disturbance of the crystal lattice. Elastic distortion and rigid rotation of the lattice are described by a unique intermediate configuration free of local stresses.

The non-local dislocation density motivated material model

The flow response for dislocation density motivated crystal plasticity modeling in a given slip system ' α ' is given by [3]:

$$\dot{\gamma}^\alpha = \begin{cases} \dot{\gamma}_0^\alpha \exp \left[\frac{-Q_{\text{slip}}}{K_B T} \left(1 - \frac{|\tau^\alpha| - \tau_{\text{pass}}^\alpha}{\tau_{\text{cut}}^\alpha} \right) \right] \text{sign}(\tau^\alpha) & \text{if } |\tau^\alpha| \geq \tau_{\text{pass}}^\alpha \\ 0 & \text{if } |\tau^\alpha| \leq \tau_{\text{pass}}^\alpha \end{cases} \quad (\text{Eqn 2})$$

where the pre-exponential variable $\dot{\gamma}_0^\alpha$ is the upper limit of the shear rate for the case where the Boltzmann factor is equal to 1, which can be found using:

$$\dot{\gamma}_0^\alpha = \frac{K_B T}{c_1 c_3 G b^2} \sqrt{\rho_P^\alpha} \quad (\text{Eqn 3})$$

and the passing stress, $\tau_{\text{pass}}^\alpha$, caused by parallel dislocations found using:

$$\tau_{\text{pass}}^\alpha = c_1 G b \sqrt{\rho_P^\alpha} \quad (\text{Eqn 4})$$

and the cutting stress, τ_{cut}^α , at 0K caused by forest dislocations is found using:

$$\tau_{cut}^\alpha = \frac{Q_{slip}}{c_2 c_3 b^2} \sqrt{\rho_F^\alpha} \quad (\text{Eqn5})$$

where Q_{slip} is the effective activation energy for dislocation slip.

The incompatibility in plastic deformation gradient and non-local geometrical non-linearity is introduced using ρ_{GND}^α which computes the geometrically necessary dislocations required to maintain continuity throughout the material. The evolution law for ρ_{GND}^α is:

$$\dot{\rho}_{GND}^\alpha = \frac{1}{b} \|\nabla_X \times (\dot{\gamma}^\alpha F_P^T) \tilde{n}^\alpha\| \quad (\text{Eqn6})$$

The material hardening at an integration point is both a function of ρ_{GND}^α and ρ_{SSD}^α (statistically stored dislocation density). The evolution laws for ρ_{SSD}^α are generally linear in shear rate (Eqn7).

$$\dot{\rho}_{SSD}^\alpha = c_4 \sqrt{\rho_F^\alpha} \dot{\gamma}^\alpha - c_5 \rho_{SSD}^\alpha \dot{\gamma}^\alpha + c_6 d_{dipole}^\alpha \rho_{mobile}^\alpha \dot{\gamma}^\alpha - c_7 \exp\left(-\frac{Q_{bulk}}{K_B T}\right) \frac{|\tau^\alpha|}{K_B T} (\rho_{SSD}^\alpha)^2 (\dot{\gamma}^\alpha)^{c_8} \quad (\text{Eqn7})$$

Global and Local Solution Strategies

The overall solution strategy algorithm is as follows:

Set $\mathbf{u}_0 = \mathbf{u}_k, \mathbf{F}_{p0} = \mathbf{F}_{pk}, \rho_{SSD,0}^\alpha = \rho_{SSD,k}^\alpha, \rho_{GND,0}^\alpha = \rho_{GND,k}^\alpha$ where \mathbf{u}_0 and \mathbf{u}_k are the displacement variable at the beginning of current increment and at the end of the last converged increment (k^{th} iteration) respectively.

(A) Load steps $k=0,1,\dots,k_{\max}$

(B) Iteration from $i=0,1,\dots,i_{\max}$

(I) Determine $\tau_i^\alpha, \mathbf{F}_{pi}$, and $\rho_{SSD,i}^\alpha$ with $\rho_{GND}^\alpha = \rho_{GND,k}^\alpha$ via local iteration at integration points

(II) Determine $\mathbf{Q}(\mathbf{u}_i, \lambda_k), \mathbf{K}_T(\mathbf{u}_i)$ and solve $\mathbf{K}_T(\mathbf{u}_i) \Delta \mathbf{u} = -\mathbf{Q}(\mathbf{u}_i, \lambda_k)$

(III) $\mathbf{u}_{i+1} = \mathbf{u}_i + \Delta \mathbf{u}_{i+1}$

(IV) Determine \mathbf{Q}^α on all nodes via patch projection

calculate $\rho_{GND,k+1}^\alpha = \rho_{GND,0}^\alpha + \Delta \rho_{GND,k}^\alpha$ on all integration points

(V) Check convergence

• if $|\rho_{GND,i}^\alpha - \rho_{GND,i+1}^\alpha| \leq tol$ \forall integration points and $|\mathbf{Q}(\mathbf{u}_{i+1})| \leq tol$

then

$\rightarrow \mathbf{u}_{k+1} = \mathbf{u}_{i+1}$,

$\rightarrow \mathbf{F}_{pk+1} = \mathbf{F}_{pi+1}, \rho_{SSD,k+1}^\alpha = \rho_{SSD,i+1}^\alpha, \rho_{GND,k+1}^\alpha = \rho_{GND,i+1}^\alpha,$

$\rightarrow k = k+1$, and

```

→ goto (A)
•else  $i=i+1$  and goto (I)

```

For each iteration ‘k’ of the current increment, the integration procedure is performed for fixed $\rho_{GND,k}^\alpha$. If the convergence criteria in step (V) are fulfilled the state variables are updated and the next load step is calculated.

Results and Discussion

Process Boundary Conditions

The applied boundary conditions in UC are shown in Figures 2 & 3. The contact boundary conditions (Figure3) with coulomb friction can be found from the literature. [5]

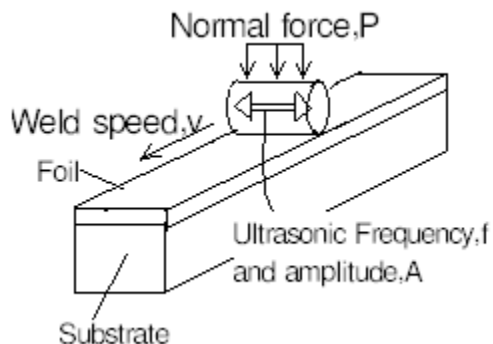


Figure2: Macroscopic Boundary conditions

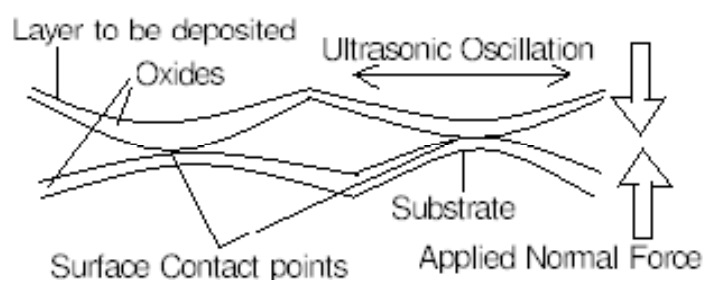


Figure3: Virgin layer and substrate scenario

Model Results

The model has been tested while predicting the joining behavior of Al 3003 H18 thin sheet with thickness dimension of 150 μm on a substrate of the same material. For all practical purposes, the thickness dimension of the substrate has been assumed to be 1mm [6] and then a representative volume element (RVE) has been generated with dimensions of 2mmx1.15mmx2mm as shown in figure 4. As shown in figure 4, the finite element mesh for deformation analysis has been made finer near the interface ($\sim 5\mu\text{m}$ length in the loading direction) since it has a very high amount of rigidity to dislocation motion due to high interfacial energy which will further lead to huge deformation gradients between the interface and the bulk material. Other input parameters were applied uniform normal pressure of 25 MPa [6], ultrasonic sinusoidal wave with Amplitude of 16 μm and frequency of 20 kHz. The deformation behavior has been analyzed for one cycle since the model is accurate to the order of dislocation content and their mesoscopic interactions and due to its computational cost. Material parameters for the constitutive model at the integration point level have been included in Table 1 [3]. Parameters which have been ignored in the current study are weld speed (v), partial contact between sonotrode and Al3003 H18 foil and between H18 foil and H18 substrate. These parameters will soon be included for better accuracy in results.

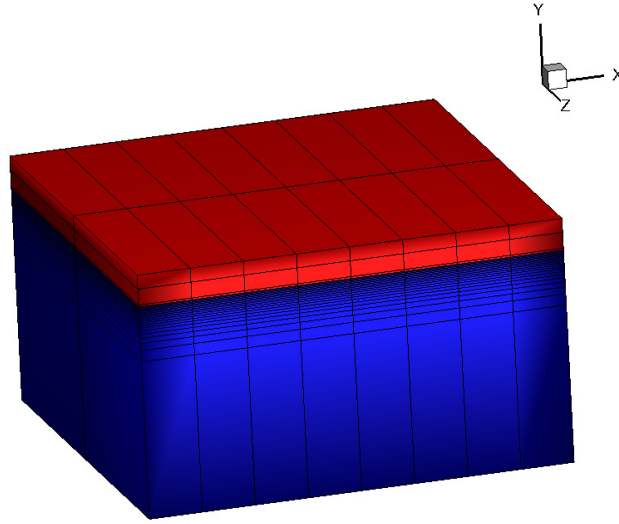


Figure4: FE Model for simulating the Ultrasonic consolidation process conditions for Al3003 H18 alloy. Red color denotes the foil and the blue color denotes the substrate. Substrate dimensions are 2mmx1mmx2mm and foil dimensions are 2mmx150 μ m x2mm

The objective of this study is to understand the interface characteristics between the substrate and the foil. The substrate-foil interface conditions have been modeled by computing the average frictional energy stored at the interface per unit of time, which equals 1.912×10^{-9} J/time step. Since the element size of the FE model near the interface is 10^3 times bigger than the actual interface length ($\sim b = 10^{-10}$ m), the energy stored at the interface is scaled to 1.912×10^{-12} J/time step. The component of this energy in the slip direction gets added to the activation energy barrier required for the dislocation slip, Q_{slip} ($\sim 3 \times 10^{-19}$ J/time step) for all the integration points sharing the interface. This has been compared to a normal metallic interface for example a grain boundary ($\sim 1/2 G b^3 \sim 6.65 \times 10^{-19}$ J/time step) which is scaled (6.65×10^{-22} J/time step) and resolved in the slip direction and the deformation behavior has been observed.

<u>Material Parameter</u>	<u>Physical Meaning</u>	<u>Prescribed Value</u>
Q_{slip}	Energy barrier for slip	3.0×10^{-19} J
Q_{bulk}	Energy barrier for climb (activated at higher temperatures)	2.4×10^{-19} J
c1	Constant for passing stress (due to in-plane dislocations) (Eqn3)	0.1
c2	Constant for Jump width (Eqn4)	2.0
c3	Constant for obstacle width (Eqn4)	1.0
c4	Constant for lock forming rate (Eqn7)	1.5×10^7 m ⁻¹
c5	Constant for athermal annihilation rate (Eqn7)	10.0
c6	Constant for thermal annihilation rate (Eqn7)	1.0×10^{-30} m ⁻¹
c7	Constant of dipole forming rate (Eqn7)	1.0×10^7 m ⁵ s ^{c8}
c8	Constant for non-linear climb of edge dislocation (Eqn7)	0.3
c9	Constant for energy scaling at the interface	10^{-3}

It has been seen with progressive deformation that the interface with frictional contact between the substrate and the foil experiences a bigger magnitude of the geometrically necessary dislocations in the edge dislocation normal direction by a factor of 100 times.

From a physical viewpoint, a higher density of geometrically necessary dislocations in the edge normal dislocation direction means that each mobile dislocation of edge nature on its slip plane experiences a higher resistance to its motion leading to their immobile accumulation and resistance to slip plane rotation at the interface (figure 5). Therefore, a higher geometrically necessary dislocation density along the frictional interface compared to the grain boundary interface leads to its grain fragmentation in the current and later cycles. The region of grain fragmentation could be identified as the thin regime in red color after 3/4th and 1 complete cycle of the deformation is complete (figure 6, right). The thickness of this regime is 2 mesh layers in the loading direction or 10 μm which matches with the grain fragmentation regime in [1] Moreover, the yield and the stress-strain curves in both the cases are identical (~160MPa (initial), figure 7) because in the small strain regime, it is only a function of the statistically stored dislocation density which measures the multiplication of initially frozen dislocations which are trapped in the material in the *as received* condition. Since the initial stored statistical density is $\sim 10^{14}/\text{m}^2$ and the maximum absolute change observed during progressive deformation is no larger than $\sim 10^5/\text{m}^2$, therefore a change in the yield stress has not been seen when the frictional contact has been compared to the grain boundary interface.

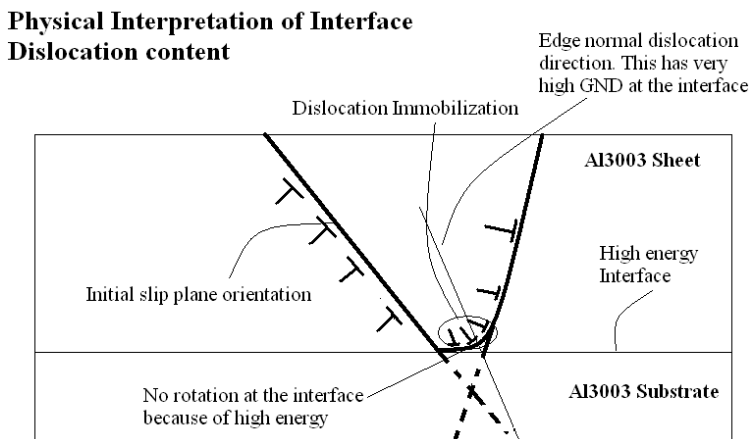
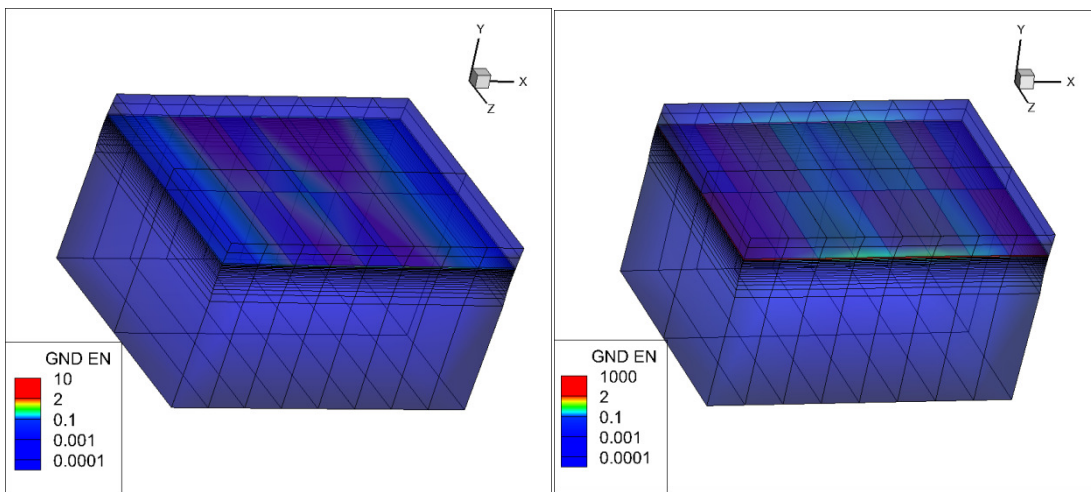
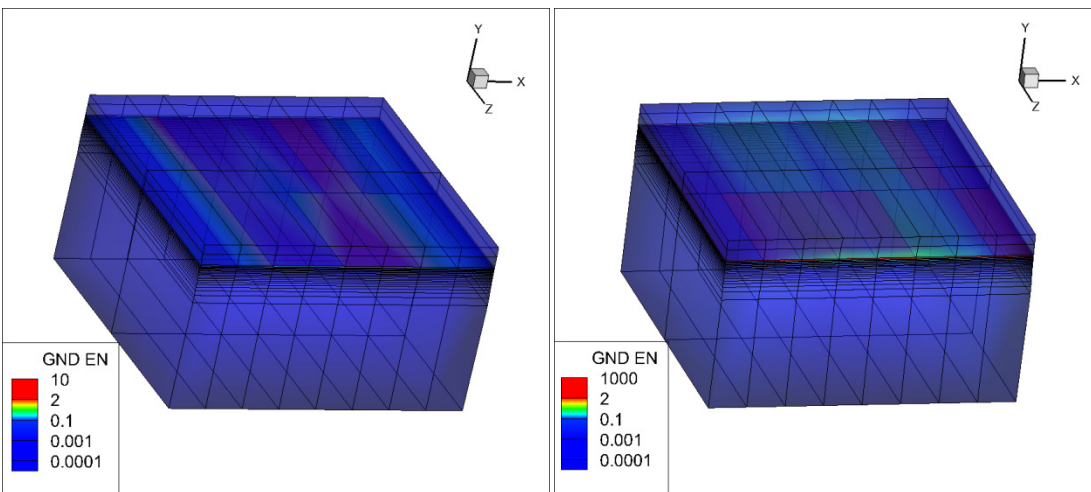


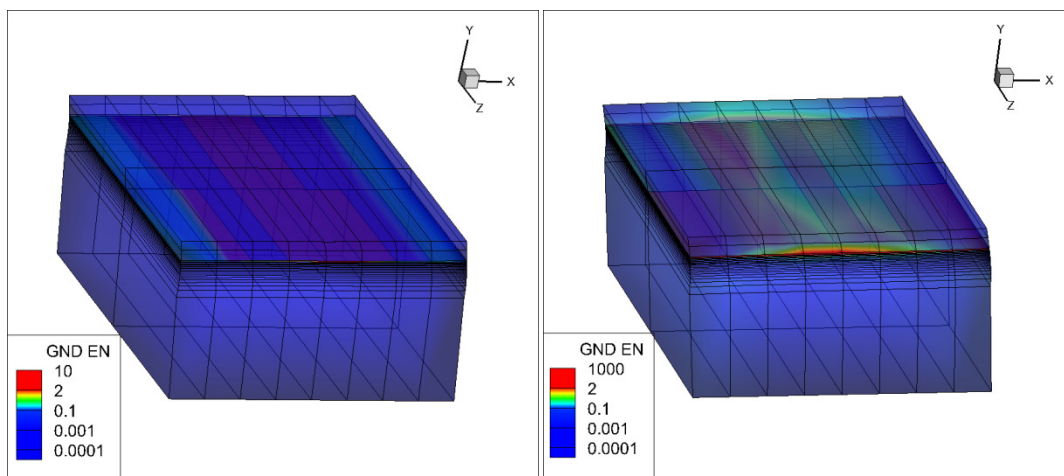
Figure5: Physical interpretation of dislocation content at the interface



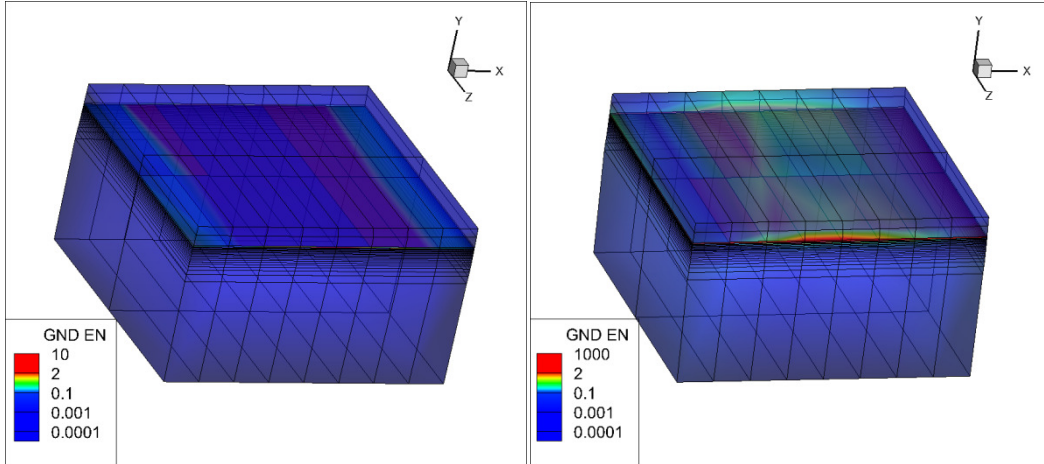
T=1/4 Cycle



T=1/2 Cycle



T=3/4 Cycle



T=1 cycle.

Figure6: The edge normal dislocation evolution at the H18-H18 interface. Pictures at left indicate grain boundary interface and pictures at right indicate the friction boundary interface. Clearly, the rotation restricting dislocation content at the interface is 100 times stronger in the frictional case than in the grain boundary case. This further leads to grain fragmentation.

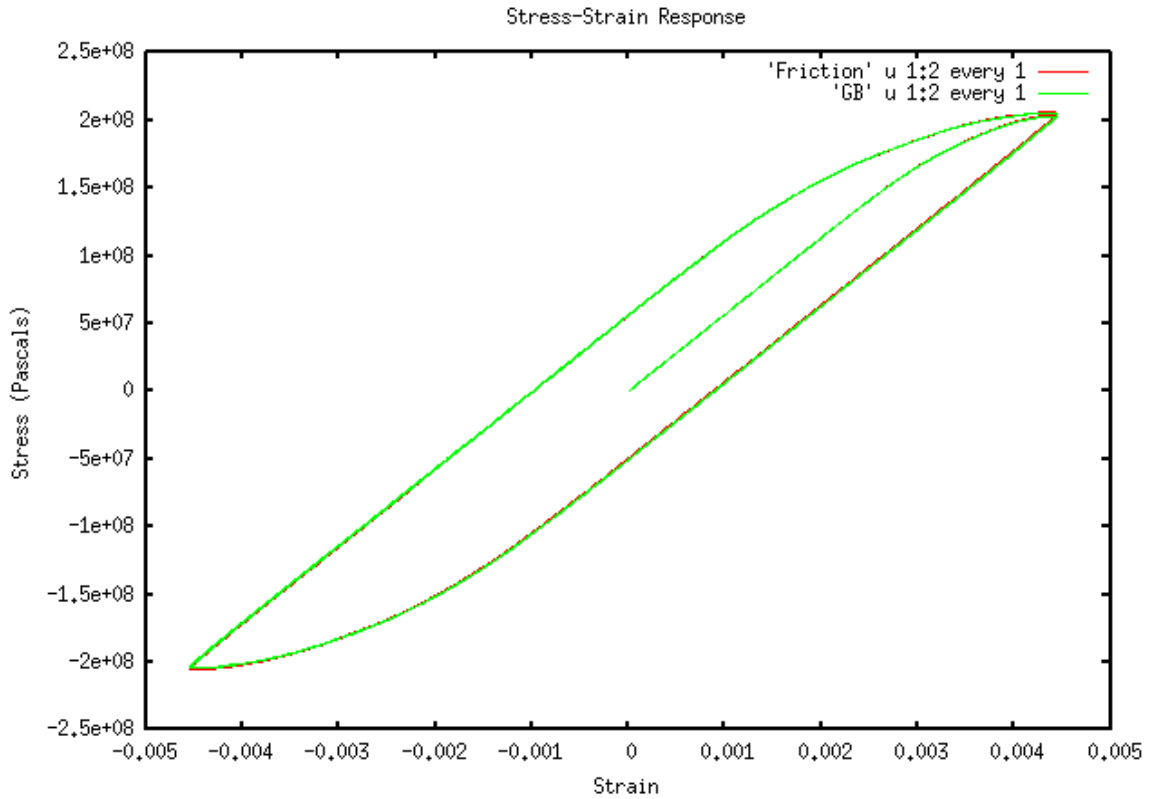


Figure7: The stress-strain responses of the H18 substrate-H18 foil system with frictional and grain boundary interfaces in red and green respectively. Notice that in the initial regime, the behavior is primarily dictated by the statistically stored dislocation density.

Conclusions and Future work

It can be concluded from the present work that the dislocation density based non-local non-linear finite element modeling can be used to analyze the Ultrasonic Consolidation process down to the mesoscopic level and many evolutionary variables, for example plastic deformation, dislocation content and grain fragmentation, can be predicted. The downside of this analysis is the time involved for computing the variables of interest close to interface because of finer mesh size. This problem can be eradicated by a robust homogenization strategy and its mathematical framework is already under development. A detailed TEM study will be conducted to identify the material parameters as shown in Table 1 when other material systems will be joined using the UC technique. The present model will be validated against the deformation response of these material systems and then converted to a tool for predicting the deformation response of new systems and the feasibility and amount of bonding which could be achieved using the UC technique in those cases. Other regimes of research interest would be to look at better statistical mechanics based ensembles and phase field study to understand the nature of the dislocation locks produced on dislocation multiplication which further restricts their motion in the slip direction.

Once these objectives are fulfilled, the combined experimentation and computation approach towards understanding the UC technique could be used as a tool in

1. Better understanding of the effect of UC process parameters on interfacial characteristics
2. Performing analytical optimization of process parameters for a given set of materials to be bonded; dramatically reduces the need for full factorial studies of process parameters.
3. Ability to model the effects of changes in sonotrode design and
4. Predicting the suitability of new materials for UC processing.

References

1. Johnson, K. *Interlaminar subgrain refinement in ultrasonic consolidation*. Wolfson School of Mechanical and Manufacturing Engineering, Loughborough University, UK. 2008. PhD Thesis.
2. Bate, P. *Modelling Deformation Microstructure with the Crystal Plasticity Finite-Element Method*. *Philosophical Transactions: Mathematical, Physical and Engineering Sciences*, Volume 357, pp. 1589-1601.
3. Ma, A., Roters, F. and Raabe, D. *A dislocation density based constitutive model for crystal plasticity FEM including geometrically necessary dislocations*. *Acta Materialia*, Volume 54, pp. 2169-2179.
4. Asaro, R.J. and Rice, J.R., 1977. *Strain localization in ductile single crystals*. *J. Mech. Phys. Solids*, Volume 25, pp. 309–338.
5. Eck, C. and Jarušek, J. *Existence Results for Contact Problems with Coulomb Friction: A Survey*. *Inequality and Contact Problems in Mechanics*, Besançon, June 22–23, 2006.
6. Siddiq A. and Ghassemieh E. *Thermomechanical analyses of ultrasonic welding process using thermal and acoustic softening effects*. *Mechanics of Materials*, Volume 40, pp. 983-1000.